SAND2010-0009C

Poroelastic Seismic Wave Propagation Modeling of CO2 Sequestration Effects

David F. Aldridge, Hans F. Schwaiger, and Lewis C. Bartel
Geophysics Department, Sandia National Laboratories, Albuquerque, New Mexico

Introduction and Summary

Long term geologic sequestration of carbon dioxide (CO_2) is increasingly considered a viable approach for removing large amounts of excess carbon from the earth's surface environment. As CO_2 is injected into a porous subsurface formation, it displaces (or mixes with) existing *in situ* pore fluids such as brine, oil, or methane. The seismic reflection and transmission responses of the formation depend on the degree of CO_2 substitution. Additionally, geochemical reactions involving CO_2 and mineral grains alter the bulk and shear moduli of the solid constituent and/or the matrix of the porous medium. In this study, we examine full waveform, wide-angle, amplitude *vs*. offset (AVO) responses of a sandstone layer. Synthetic seismic data are calculated with a 3D poroelastic wave propagation algorithm that solves Biot's governing system of 13 coupled partial differential equations via an explicit, time-domain, finite-difference method. All of the common seismological phases (primary and multiple reflections, mode conversions, head waves, surface and interface waves, etc.) are generated with fidelity, provided spatial and temporal intervals are sufficiently fine.

Initial calculations indicate that full or partial replacement of H_2O by CO_2 is readily detected by the AVO recording configuration, particularly with the long offset shear events. Difference seismogram amplitudes of surface-recorded multi-component particle velocities range up to 25%. A sharp CO_2/H_2O front generates weak diffractions that may not be readily detected by AVO recording. Poroelastic sensitivity modeling experiments of this type need to be extended to carbonate layer geology, higher spectral bandwidths, and a vertical seismic profiling (VSP) acquisition configuration.

Earth Model and Reflection AVO Data Acquisition Configuration

Earth Model: a homogeneous porous sandstone layer (25 m thick) overlain and underlain by homogeneous shales. Top of layer is 250 m below horizontal stress-free surface.

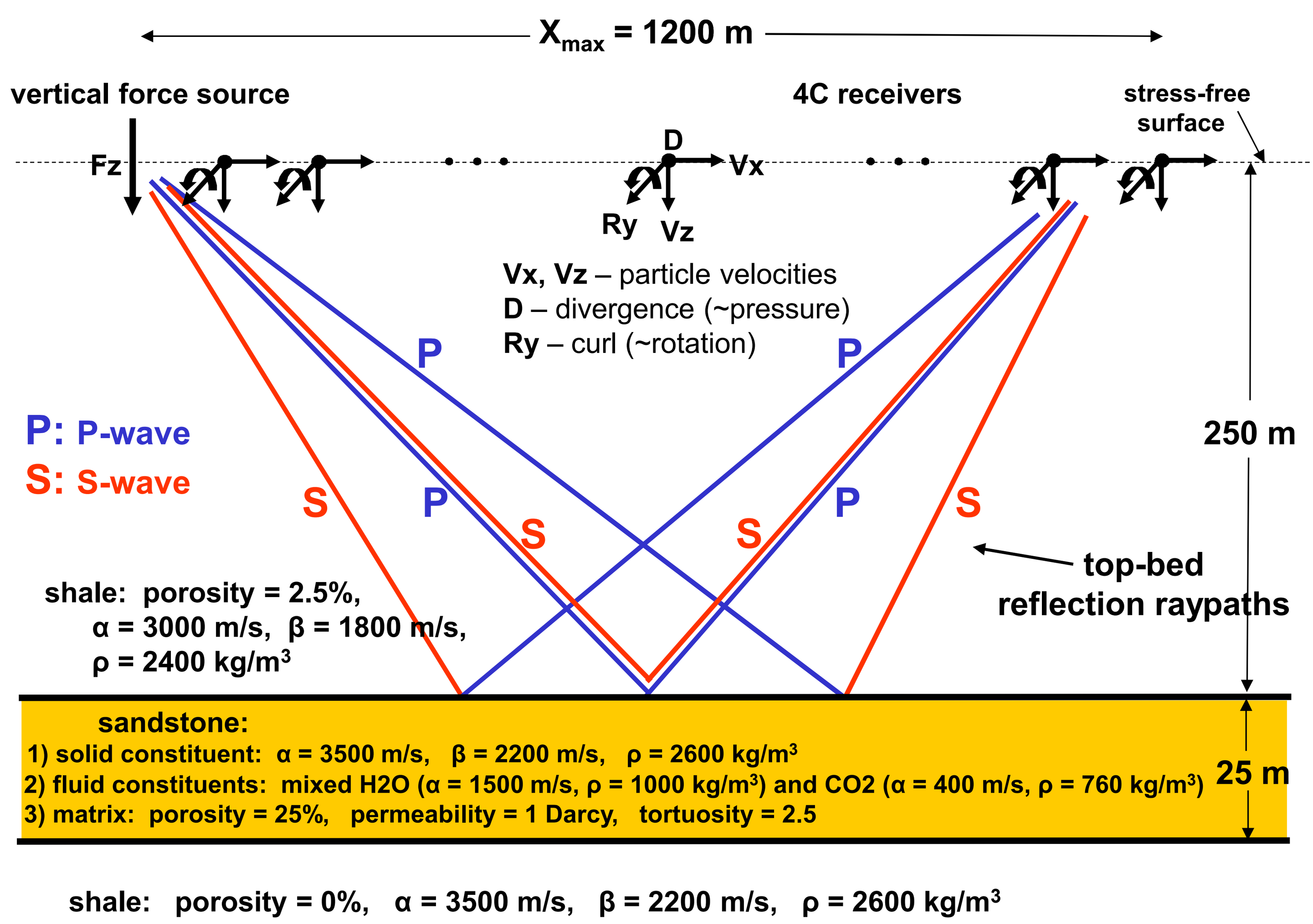

Data Acquisition Geometry:

1) Vertical force source applied to stress-free surface (mimics Vibroseis source acquisition). Source pulse is 30 Ricker wavelet.
2) Four-component (4C) receivers deployed on surface record inline horizontal and vertical particle velocities, crossline particle rotation, and displacement divergence.
3) Maximum source-receiver offset of 1200 m simulates wide-angle AVO recording (offset-to-depth ratio ~5:1).

Acknowledgements

Aspects of the research reported here are supported by the New Mexico Small Business Assistance Office of Sandia National Laboratories, and working in collaboration with the Roswell, New Mexico firm Providence Technologies Inc. (Mr. James C. Manatt, Jr., CEO). Providence Technologies is involved in exploration and production of petroleum resources in the Permian Basin of Texas and New Mexico.

Sandia National Laboratories is a multiprogram science and engineering facility operated by Sandia Corporation, a Lockheed-Martin Company, for the US Department of Energy's National Nuclear Security Administration, under contract DE-AC04-94AL85000.

Poroelastic Wave Equations and 3D Finite-Difference Grid

Thirteen, coupled, first-order, non-homogeneous, partial differential equations:

$$\rho_{11}\frac{\partial \mathbf{v}_s}{\partial t}+\rho_{12}\frac{\partial \mathbf{v}_f}{\partial t}+b(\mathbf{v}_s-\mathbf{v}_f)-(1-\phi)\nabla\cdot\boldsymbol{\sigma}=(1-\phi)\left(\mathbf{f}_s+\nabla\cdot\mathbf{m}_s^{asym}\right)$$

$$\rho_{12}\frac{\partial \mathbf{v}_s}{\partial t}+\rho_{22}\frac{\partial \mathbf{v}_f}{\partial t}-b(\mathbf{v}_s-\mathbf{v}_f)+\phi\nabla p=\phi\left(\mathbf{f}_f+\nabla\cdot\mathbf{m}_f^{asym}\right)$$

$$(1-\phi)\frac{\partial \boldsymbol{\sigma}}{\partial t}-A(\nabla\cdot\mathbf{v}_s)\mathbf{I}-Q(\nabla\cdot\mathbf{v}_f)\mathbf{I}-\mu\left(\nabla\mathbf{v}_s+\nabla\mathbf{v}_s^T\right)=\frac{\partial \mathbf{m}_s^{sym}}{\partial t}$$

$$\phi\frac{\partial p}{\partial t}+Q(\nabla\cdot\mathbf{v}_s)+R(\nabla\cdot\mathbf{v}_f)=-\frac{\phi}{3}\frac{\partial}{\partial t}\mathrm{Tr}\{\mathbf{m}_f^{sym}\}$$

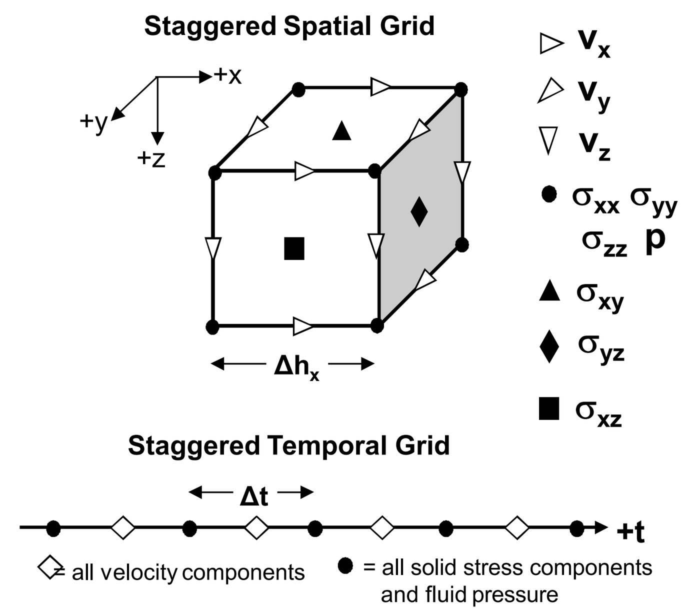

Wavefield Variables:
- $\mathbf{v}_s(\mathbf{x},t)$ – solid velocity vector
- $\mathbf{v}_f(\mathbf{x},t)$ – fluid velocity vector
- $\sigma(\mathbf{x},t)$ – solid stress tensor
- $p(\mathbf{x},t)$ – fluid pressure

Poroelastic Earth Model Parameters:
- $\phi(\mathbf{x})$ – porosity
- $\rho_{11}(\mathbf{x})$, $\rho_{12}(\mathbf{x})$, $\rho_{22}(\mathbf{x})$ – inertial coupling coefficients
- $b(\mathbf{x})$ – viscous coupling coefficient
- $A(\mathbf{x})$, $Q(\mathbf{x})$, $R(\mathbf{x})$ $\mu(\mathbf{x})$ – moduli

Seismic Body Sources:
- $\mathbf{f}_s(\mathbf{x},t)$ – solid force density vector
- $\mathbf{f}_f(\mathbf{x},t)$ – fluid force density vector
- $\mathbf{m}_s(\mathbf{x},t)$ – solid moment density tensor
- $\mathbf{m}_f(\mathbf{x},t)$ – fluid moment density tensor

This 3D ***velocity-stress-pressure*** system is numerically solved with an explicit, time-domain, staggered-grid, O(2,4) finite-difference algorithm.

Advantage: Wave propagation physics in two-phase media is properly accounted for. No need to resort to "effective elastic medium" representation of a fluid-saturated porous body.

Disadvantage: Computational cost, in terms of memory and execution time, is significantly greater thean for isotropic elastic modeling. There are *thirteen* dependent variables and *nine* medium parameters.

CO2 Injection Front Model

CO2 / H2O front located 500 m from injection well at 0 m

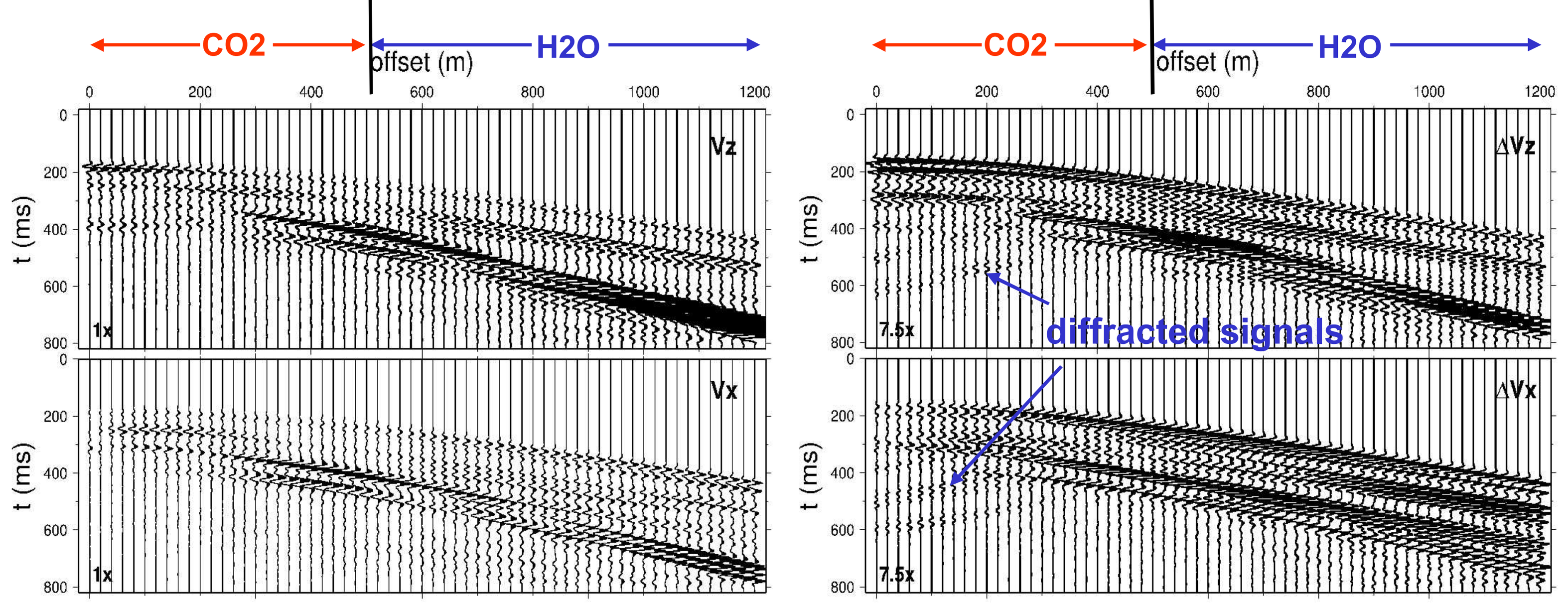

Vertical and inline horizontal particle velocity traces, plotted at 1X gain, give *no* indication of CO2 front!

Difference traces, obtained by subtracting off responses for uniform H2O saturation, reveal weak diffractions emanating from CO2 front. Note 7.5x plot gain compared to left panel.

Actual CO2 / H2O front will be diffuse rather than sharp, indicating that diffraction signals will be even weaker! Hence, reflection AVO configuration may not be able to resolve front location well.

Uniformly Saturated Sandstone Layer Model

Particle Velocity Responses

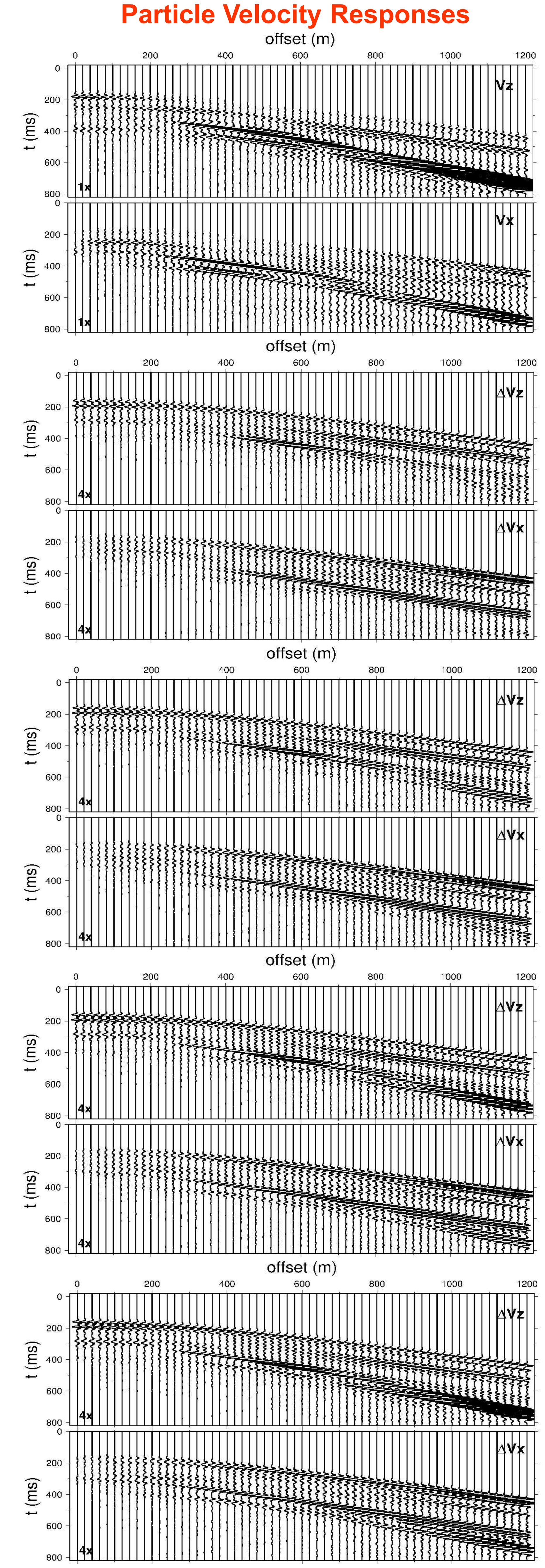

AVO responses for

100% H2O (= 0% CO2) saturation

(direct and surface waves removed by subtraction)

Difference AVO responses (plotted with 4x gain relative to 1x above)

100% H2O minus 25% CO2

AVO responses consist of top-bed and bottom-bed primary reflections (PP, PS, SP, SS), together wih all orders of intrabed multiples.

100% H2O minus 50% CO2

Divergence and rotation receivers tend to isolate P and S arrivals, respectively.

100% H2O minus 75% CO2

Amplitude of difference traces are ~ 1/4 of amplitude of reference traces (100% H2O).

100% H2O minus 100% CO2

Note increasing amplitude of wide-angle AVO responses (particularly SS event) as CO2 replaces H2O.

Divergence / Rotation Responses